

**Structure-Function Studies of
Ribulose-1,5-bisphosphate
Carboxylase/Oxygenase: Activation,
Thermostability, and CO₂/O₂
Specificity**

Saeid Karkehabadi

*Faculty of Natural Resources and Agricultural Sciences
Department of Molecular Biology
Uppsala*

**Doctoral thesis
Swedish University of Agricultural Sciences
Uppsala 2005**

Acta Universitatis Agriculturae Sueciae

2005: 28

ISSN 1652-6880
ISBN 91-576-7027-7
© 2005 Saeid Karkehabadi, Uppsala
Tryck: SLU Service/Repro, Uppsala 2005

Abstract

Karkehabdi, S., 2005. Structure-Function Studies of Ribulose-1,5-bisphosphate Carboxylase/Oxygenase: Activation, Thermostability, and CO₂/O₂ Specificity. Doctoral dissertation.

ISSN 1652-6880, ISBN 91-576-7027-7.

Rubisco (ribulose 1,5-bisphosphate carboxylase/oxygenase) catalyses the CO₂ fixation of photosynthesis. Despite its central role for life, Rubisco is inefficient and is subject to competitive inhibition by O₂. This makes Rubisco a target for mechanistic studies and engineering, requiring a detailed knowledge of the molecular basis for its catalysis and specificity. Rubisco from higher plants consists of eight large, and eight small subunits. This thesis investigates the role of structural elements of Rubisco, spanning from the active site on the large subunit to the small subunit and the subunit interfaces.

The structure of Rubisco with a calcium ion in place of the native magnesium activator ion illustrates how the catalytic properties depend on the nature of the metal ion. The larger radius of the calcium ion and its reduced Lewis-acid character causes increases in certain metal-ligand distances, and could explain why calcium does not support catalysis. The mutation C172S in the active site was shown to simultaneously improve specificity and influence the redox-stability of Rubisco.

Analysis of mutations (V331A, T342I) in a mobile loop (Loop 6) of the large subunit illustrates the importance of a precise geometry of the loop for catalytic efficiency and specificity. The substitution D473E at the C-terminus is shown to disrupt a network of hydrogen bonds relayed to Loop 6 and to cause disorder of the C-terminus. This may explain the reduced specificity of this mutant. Mutations at the interface of the large and small subunits also influence the stability and catalytic efficiency. Analysis of temperature factors in the structures of L290F and L290F/A222T pinpoints the regions of instability and suggests how the effect is reversed by one single mutation. The influence of interactions at the subunit interface on catalysis was analysed by replacement of the small-subunit β A- β B loop of *Chlamydomonas* Rubisco with the corresponding loops of *Synechococcus* (ABAN) and spinach (ABSO) Rubisco. The structures show a significant interaction area of the β A- β B loop in ABAN is lost, leading to reduced catalytic efficiency and specificity, whereas the total loop-interaction area in ABSO is similar to that in the spinach or wild-type enzymes.

Keywords: Rubisco, thermal stability, CO₂/O₂ specificity, site-directed mutagenesis, crystal structures, *Chlamydomonas reinhardtii*.

Author's address: Saeid Karkehabadi, Department of Molecular Biology, SLU, S-751 24 Uppsala, Sweden

To my family: Faranak, Behrad and Vida

Contents

1. Background	9
1.1 Rubisco is essential for life on earth	9
1.2 Rubisco is a bi-functional enzyme	9
1.3. Regulation of activity	10
1.3.1 Activation	10
1.3.2 Activase-mediated activity	10
1.3.3 Redox regulation	11
1.4 Topics for research	11
1.5 Three-dimensional structure of Rubisco	12
1.5.1 Quaternary structure	12
1.5.2 Tertiary structure	13
1.5.3 Interactions between large and small subunits	13
1.5.4 The active site	15
1.5.5 Conformational changes	15
1.6 Mutagenesis studies	16
1.6.1 <i>Chlamydomonas reinhardtii</i> serves as a model system for the study of Rubisco	16
1.6.2 The molecular bases for most mutants are still unexplored	17
2. The aim of this thesis	19
3. Methods	20
3.1 Cell growth, purification and crystallization	20
3.2 X-ray crystallography	20
3.3 Molecular replacement	21
3.4 Non-crystallographic symmetry	22
3.5 Temperature factors	22
3.6 Merohedral twinning	22
4. Results and discussion	24
4.1 The active site and the role of the metal ion	24
4.2 The redox state of cysteine 172 influences Rubisco's activity and susceptibility to degradation	25
4.2.1 Substitution of Cys172 by serine increases the CO ₂ /O ₂ specificity	25
4.2.2 Structural changes induced by the C172S substitution	25
4.3 Elements involved in the dynamics of catalysis	26
4.3.1 Mutation at the base of Loop 6 influence the CO ₂ /O ₂ specificity	27
4.3.2 Importance of the C-terminus	27
4.4 Interactions at the interface of large and small subunits influence stability and catalytic ability of Rubisco	28
4.4.1 Leucine 290, a critical residue at the interface of large and small subunits	28

<i>4.4.2 Temperature factors carry valuable information about the stability of the enzyme</i>	29
<i>4.4.3 Disorder may be transmitted to the active site via long-range interactions</i>	31
<i>4.4.4 The βA-βB loop makes major contributions to the stability of the enzyme</i>	32
<i>4.4.5 Comparison of structures of ABAN, ABSO and wild-type Chlamydomonas Rubisco</i>	33
<i>4.4.6 Interactions at the subunit interface influence the thermal stability of Rubisco</i>	34
<i>4.4.7 Arg59 and Arg71 are critical residues at the interface of large and small subunit</i>	35
5. Future perspectives	37
6. References	39
7. Acknowledgements	44

Appendix

Papers I-V

This thesis is based on the following papers, which will be referred to by their Roman numerals:

I. Karkehabadi, S., Taylor, T.C & Andersson, I. (2003). Calcium supports loop closure but not catalysis in Rubisco. *J. Mol. Biol.* **334**, 65-73.

II. Karkehabadi, S., Taylor, T.C., Spreitzer, R.J. & Andersson, I. (2005). Altered intersubunit interactions in crystal structures of catalytically compromised ribulosebiphosphate carboxylase/oxygenase. *Biochemistry*, **44**, 113-120

III. Karkehabadi, S., Peddi, S.R., Anwaruzzaman, Md., Cederlund, A., Andersson, I. & Spreitzer, R.J. Evolutionary divergence in the structure of the small-subunit β A- β B loop of ribulosebiphosphate carboxylase/oxygenase does not hinder assembly but influences large-subunit catalysis. Manuscript.

IV. Garcia, M. J., Karkehabadi, S., Spreitzer, R.J., Andersson, I. & Moreno, J. Structural and functional consequences of the substitution of vicinal residues Cys172 and Cys192 in the large subunit of ribulose 1,5-bisphosphate carboxylase/oxygenase from *Chlamydomonas reinhardtii*. Manuscript.

V. Karkehabadi, S., Taylor, T.C., Spreitzer, R.J. & Andersson, I. Structural analysis of altered large-subunit carboxy-terminus/loop-6 interactions that influence catalytic efficiency and CO₂/O₂ specificity of ribulose 1,5-bisphosphate carboxylase/oxygenase. Manuscript.

Papers I and II are reproduced by permission of the journal

1. Background

1.1 Rubisco is essential for life on Earth

Ribulose 1,5-bisphosphate carboxylase/oxygenase (Rubisco) is the primary carboxylating enzyme used by all photosynthetic organisms to incorporate atmospheric CO₂ into carbohydrate needed for growth and development. Nearly all of the carbon atoms that are present in living organisms have passed through the active site of Rubisco. The most abundant enzyme on Earth, Rubisco is universally present in all of the Earth's vegetation and in microorganisms on land and in the ocean. It comprises around 40% of the total protein of the plant. Hence, Rubisco represents an enormous sink for nitrogen and other valuable resources within plants.

1.2 Rubisco is a bifunctional enzyme

Carboxylation, which is the main reaction catalyzed by Rubisco, involves the addition of CO₂ to a molecule of a five-carbon sugar substrate, ribulose-1,5-bisphosphate (RuBP) to produce two molecules of 3-phosphoglycerate (3PGA). This reaction can be dissected into several partial reactions (Taylor & Andersson, 1997; Cleland *et al.*, 1998) (Figure 1.1). 1) Enolization; abstraction of a proton from C-3 of the substrate results in the formation of the 2,3-enediol intermediate. 2) Carboxylation; the addition of CO₂ to the 2,3-enediol generates a 6-carbon intermediate, 2-carboxy-3-keto-arabinitol-1,5-bisphosphate (CKABP). 3) Hydration; the hydration of CKABP yields the gemdiol form of the ketone. 4) Carbon-carbon bond cleavage; deprotonation of the gemdiol leads to carbon bond scission and results in formation of one molecule of 3PGA and one molecule of 3PGA in the form of carbanion. 5) Protonation; the carbanion is protonated and the second molecule of 3PGA is formed.

Rubisco, however, is a bifunctional enzyme that also possesses an oxygenation activity. In this reaction, the sugar substrate is oxygenated to produce one molecule of 3PGA and one molecule of 2-phosphoglycolate. The latter product is the substrate for photorespiration. Photorespiration results in loss of carbon and energy from plant tissues. (Bowes *et al.*, 1971; Ogren & Bowes, 1971; Lorimer, 1981). CO₂ and O₂ compete for the same active site on Rubisco to drive photosynthesis and photorespiration respectively.

The ratio of carboxylation to oxygenation at any specified concentrations of CO₂ and O₂ is referred to as the CO₂/O₂ specificity factor, Ω (or τ) = $V_c K_o / K_c V_o$ where V_c and K_c are the maximum velocity and the Michaelis constant for carboxylation, and V_o and K_o are the maximum velocity and the Michaelis constant for the oxygenation reaction. There is natural variation in the catalytic efficiency of Rubisco from diverse species. Substrate specificity is approximately 15 in photosynthetic bacteria, 50 in cyanobacteria, 60 in green algae, 80 in higher plants and about 200 in thermophilic red algae.

A number of regions in the structure of the enzyme have been identified (reviewed in Spreitzer, 1993) that may account for this variation. This suggests that it may be possible to engineer a more efficient enzyme.

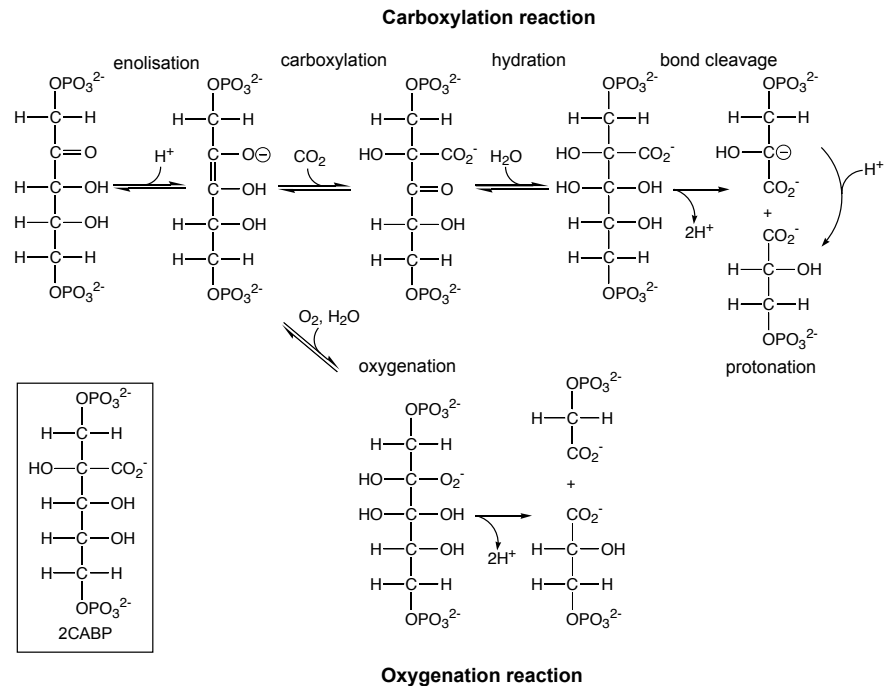


Figure 1.1 Reaction pathways for carboxylation and oxygenation catalyzed by Rubisco. 2CABP is an analogue of the gem-diol intermediate prior to bond cleavage.

1.3 Regulation of activity

1.3.1 Activation

Rubisco must be activated to carry out carboxylation or oxygenation. The catalytically competent form of the enzyme is a complex of enzyme- $\text{CO}_2\text{-Mg}^{2+}$, in which the molecule of CO_2 is different from the substrate CO_2 . The first step in the activation process is carbamylation by CO_2 at an uncharged amine of a lysine residue (Lys201, the numbering is based on the sequence of the spinach enzyme) in the active site of Rubisco. The resulting carbamate is anionic and is capable of binding a Mg^{2+} ion (Lorimer & Miziorko, 1980) which stabilizes the carbamate. This completes the activation process.

1.3.2 Activase-mediated activation

The tight binding of ribulose-1,5-bisphosphate to uncarbamylated enzyme molecules displaces the equilibrium to a dead-end binary complex, Rubisco-RuBP), so that the rate of reaction declines and eventually stops.

Ogren and colleagues recovered a mutant of *Arabidopsis thaliana*, which was deficient in Rubisco activation even at high light intensity, and high concentrations of CO₂ (Sommerville *et al.*, 1982). Surprisingly, the Rubisco activity of this mutant *in vitro* appeared to be indistinguishable from the wild-type enzyme. These contradictory results led to the discovery of Rubisco activase. It was subsequently shown that the activase is not directly involved in carbamylation, thus it is not a carbamylase, but dissociates RuBP from decarbamylated active sites and consequently promotes the access of CO₂ and Mg²⁺ for the carbamylation of the enzyme.

Rubisco activase from many species has been purified and its primary structure, ATPase activity and the relationship between its oligomeric structure and activity have been studied. However, very little is known about the mechanism by which activase promotes dissociation of ligands bound to the uncarbamylation complex.

Rubisco activase in higher plants is composed of two monomeric isoforms of 41-43 and 45-46 kD respectively (Robinson & Portis, 1989), which may have different catalytic properties. The size of the mature protein varies between 280 and 600 kD. This variation depends highly on the concentration of Mg²⁺ and the adenine nucleotide present (Wang *et al.*, 1993). The oligomerization state of the activase depends also on its concentration, the smaller oligomers are formed as the protein is diluted. Rubisco activase exhibits ATP dependent activity and although the rate of Rubisco activation is enhanced as the rate of ATPase activity is increased, the ATPase activity is not directly connected to the activation of Rubisco (Portis, 1995). The specific activity of Rubisco activase towards Rubisco decreases at lower concentrations of Rubisco activase, which suggests that a large oligomer of activase is necessary for removal of sugar phosphates from unactivated Rubisco while a smaller oligomer of the activase may exhibit ATPase activity (Portis, 1995). The tertiary structure of Rubisco activase has not been determined and the mechanism by which it binds Rubisco and leads to release of the bound RuBP or the inhibitor is not understood.

1.3.3 Redox regulation

In addition to its vital role as a carboxylase, because of its abundance, Rubisco is an important source of nitrogen and other organic substances (Ellis, 1979). During nutritionally critical periods, these substances can be reutilized by degradation of Rubisco (Ferreira & Davies, 1987). It has been suggested that the redox state of one or several cysteine residues regulates activity and Rubisco's susceptibility to proteolysis (Schloss *et al.*, 1978). Experimental evidence has shown that oxidizing or reducing agents can influence the function of the enzyme through oxidation or reduction of Cys172 of the large subunit (Moreno & Spreitzer, 1999). Cys172 is a highly conserved residue and is situated in the vicinity of the active site.

1.4 Topics for research

Rubisco combines several outstanding features that have made it an attractive target for research. It is one of the largest, and also one of the most sluggish

enzymes. It cannot differentiate between CO₂ and O₂, and as a result it catalyzes both oxygenation and carboxylation of the sugar substrate RuBP. It is one of the most abundant enzymes, thus represents a significant part of the nitrogen resource and plays a fundamental role in nutritional balance during senescence of plants. Although these motivations are all significant, the main reason that this enzyme has been of considerable interest is to improve its efficiency, which would have great agronomic importance.

1.5 Three-dimensional structure of Rubisco

1.5.1 Quaternary structure

In higher plants, algae and cyanobacteria, Rubisco is built up from eight copies each of two distinct subunits (Form I Rubisco). The large (L) subunit has a molecular mass of approximately 55 kD and the small (S) subunit approximately 15 kD. Rubisco from some prokaryotes and dinoflagellates exists only as a dimer of large subunits (Form II Rubisco). There is also another form of Rubisco (Form III Rubisco) found in certain thermophilic archaea e.g. *Pyrococcus kodakaraensis*, which has a dodecameric structure with five dimers of large subunits (Maeda *et al.*, 1999).

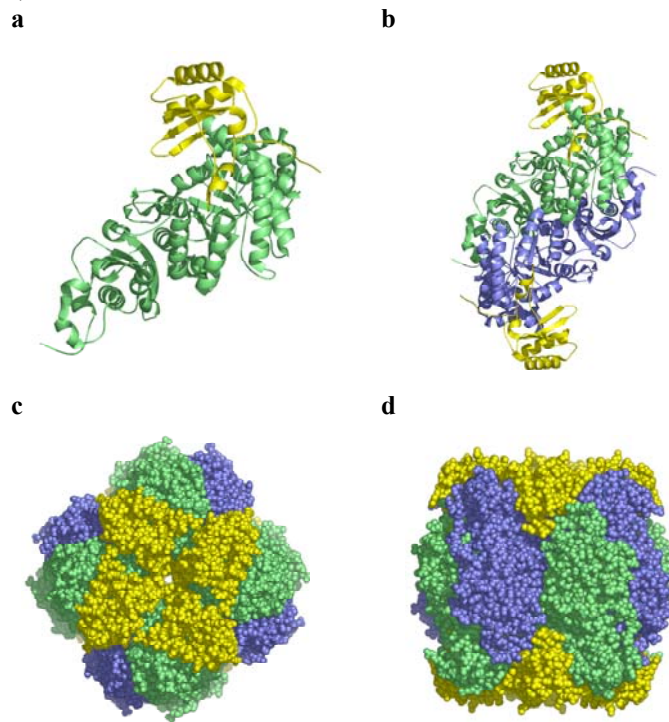


Figure 1.2 The arrangement of subunits in hexadecameric Rubisco. The L subunits are shown in green and blue and the S subunits are shown in yellow. (a) One L and one S subunit. (b) Two units of LS that are related by a 2-fold axis. (c) The complete holoenzyme (L₈S₈) viewed down to the four-fold axis. (d) The complete holoenzyme viewed perpendicular to (c).

The hexadecameric form of Rubisco has molecular 422 symmetry. Four L2 dimers are arranged around a four-fold axis and four S subunits cap the bottom and the top of the eight L subunits (Figure 1.2).

The holoenzyme can thus be described as four L2S2 units. The LS units in each of the four L2S2 units are related by a two-fold axis perpendicular to the four-fold axis. There are two active sites at the interface of each L2 dimer. A solvent channel runs along the four-fold axis. The size of this channel varies between species, this is caused by the differing size of a small-subunit loop (the β A- β B loop, see below) that lines the channel.

1.5.2 Tertiary structure

In all forms of Rubisco, the large subunit is composed of two distinct domains, an N-terminal domain, comprising residues 1-150 and a C-terminal domain, built up by residues 151-475. The C-terminal domain consists of an eight stranded α/β -barrel motif. Most of the active site residues are contributed by loops connecting the β strands and the α helices of the α/β -barrel. The remainder is donated by loops of the N-terminal domain of the large subunit of the adjacent monomer of the dimer. The small subunit, which is a four stranded anti-parallel β -sheet covered by two helices on one side, is situated far from the active site and donates no residues to the active site.

1.5.3 Interactions between large and small subunits

The small subunits are arranged as two clusters of tetramers that cover the top and the bottom of the large subunits. The minimal functional unit of Rubisco is a dimer of large subunits (L2). Although the small subunit does not contribute residues to the active site, and thus is not directly involved in catalysis, the influence of the small subunit on the catalytic reaction should not be overlooked. Removal of the small subunits from cyanobacterial Rubisco results in some 200-fold drop in V_{\max} (Andrews, 1988). Each small subunit makes interactions with three large subunits and two other small subunits. (Figure 2.2)

In general, the level of sequence homology of Rubisco from different species is much lower in the small subunit compared to the large subunit. However, some highly conserved regions stand out. One of the regions that is absolutely conserved in the small subunit of higher plants and *Chlamydomonas reinhardtii* is β strand B, comprising residues 66-82. This strand is connected to the preceding strand A (residues 39 to 45) by a hairpin loop, the β A- β B loop which has interesting features.

In *Chlamydomonas* Rubisco, the β A- β B loop contains 28 residues, whereas in land plants and cyanobacteria, the length of this loop is 22 and 9 residues, respectively. Experimental evidence indicates that this loop plays an important role in assembly (Wasman *et al.*, 1989) and thermostability (Flachman & Bohnert, 1992) of the holoenzyme. The loop is located at the entrance of the central cavity that runs along the four-fold axis of the molecule. The radius of this cavity is variable in Rubisco from different species. For instance, *Chlamydomonas*

Rubisco has a smaller cavity than spinach Rubisco because of the larger size of the β A- β B loop. The extended C-terminal of the small subunit of Rubisco in *Ralstonia eutropha* and *Galdieria partita* confers more bulk to this channel and makes it even narrower (Hansen *et al.*, 1999; Sugawara *et al.*, 1999) (Figure 2.3). The β A- β B loop is in contact with two large and two small subunits. It contributes over 20% of the buried area between the large and small subunits and makes a number of hydrogen bonds with the two neighbouring large subunits.

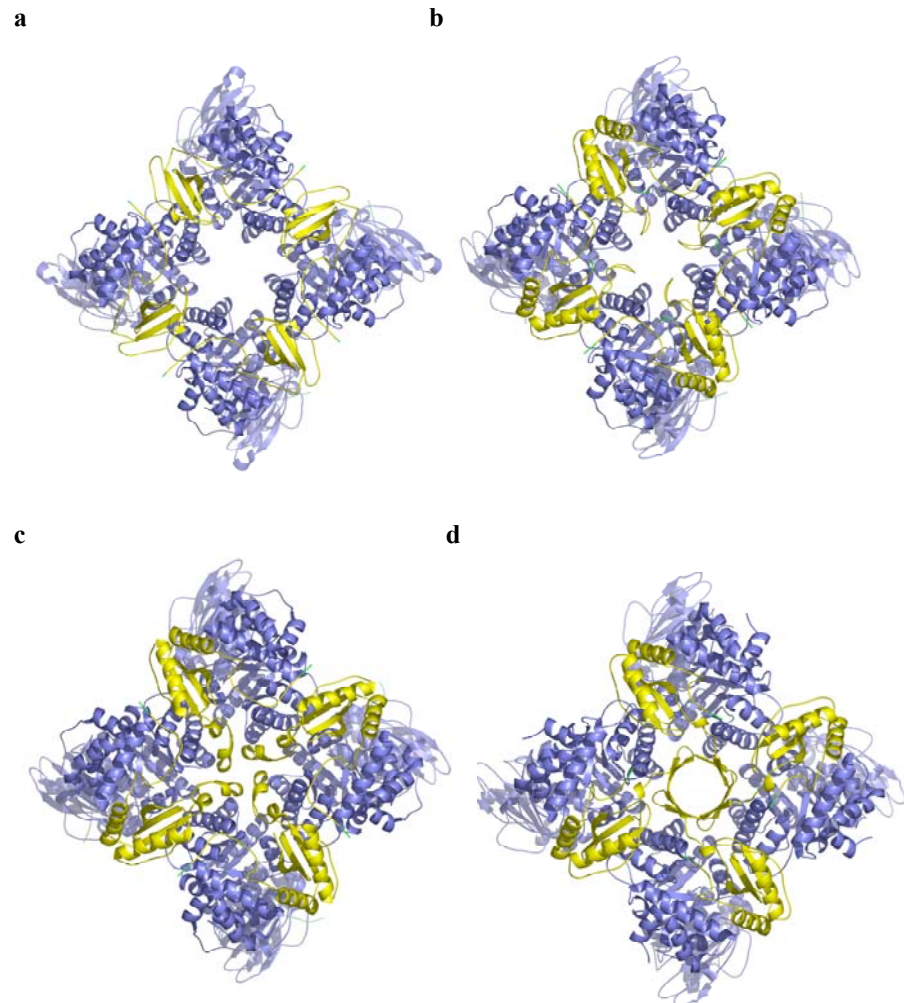


Figure 2.3 The size of solvent channel varies among Rubisco from different species. The L subunits are shown in blue and the S subunits are depicted in yellow. (a) *Synechococcus* Rubisco (b) spinach Rubisco (c) *Chlamydomonas* Rubisco, and (d) Rubisco from *Ralstonia eutropha*. In each case an L4S4 is shown.

1.5.4 The active site

The active site is at the C-terminal end of the α/β -barrel, which faces the interface of the L2 dimer. The sugar substrate binds across the opening of the barrel with the phosphate groups anchored at each side of the barrel. In the crystal structure of Rubisco complexed with the transition state analogue 2-D-carboxy-1,5-arabinitolbiphosphate, 2CABP (Andersson *et al.*, 1989; Andersson, 1996), the Mg^{2+} ion displays a nearly perfect octahedral coordination, and is ligated by six oxygen ligands (Figure 2.4). Three of them are provided by 2CABP and the other three by the carbamylated Lys201, Asp203 and Glu204. 2CABP also interacts with Lys175, Lys177 and Lys334. Lys334 sits at the tip of a loop (Loop 6) that connects strand 6 of the α/β -barrel with helix 6. Another residue which has been suggested to have a critical function in the regulation of Rubisco (Moreno & Spreitzer, 1999) is Cys172. Cys172 is situated in the vicinity of the active site and makes van der Waals interactions with Gly403. It also makes a hydrogen bond to the carbamylated lysine. In wild-type *Chlamydomonas* Rubisco the thiol group of Cys172 is about 3.9 Å away from the thiol group of another highly conserved cysteine at position 192 within the same large subunit.

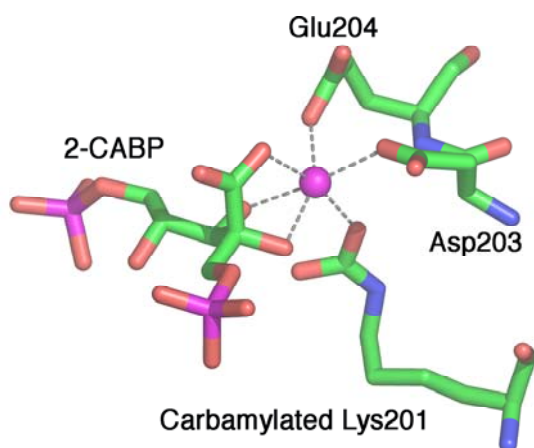


Figure 2.4 The coordination sphere of the magnesium ion is an almost perfect octahedral arrangement. Three of the ligands are provided by 2CABP and the other three by the side-chains of Asp203, Glu204 and the carbamoyl group on Lys201.

1.5.5 Conformational changes

A number of crystal structures of activated or unactivated Rubisco bound to different phosphorylated ligands such as the transition analogue 2CABP, the natural substrate RuBP, and the product 3PGA, have been determined. These structures show significant conformational changes in and around the active site.

A comparison of the structures of the activated complexes of Rubisco-2CABP with Rubisco-3PGA shows that Loop 6 (residues 331-338) of the α/β -barrel domain is moved about 12Å and extends over the active site in the former structure. By doing so, Lys334, which is situated at the tip of this loop, is brought into the active site and makes numerous interactions with the ligand. In higher plants and green algae, most of the Loop 6 residues are strictly conserved. Mutational studies have revealed that alterations in this loop have deleterious effects on the catalytic properties of the enzyme. The movement of Loop 6, from the open to closed form, involves a critical amino acid, Val331. This residue, which is also highly conserved, is situated in the N-terminal end of the loop and is part of a hinge upon which the rotation takes place (Newman & Gutteridge, 1993).

Other changes include the N-terminal domain and the positioning of the 60s loop, residues 60-66, over the active site. In addition to hydrogen bonds with the ligand, Lys334 makes hydrogen bonds with Glu60 and Thr65 of the 60s loop of the adjacent large subunit (Knight *et al.*, 1990).

A third region that becomes ordered is the C-terminus of the large subunit. This region, comprising residues 467-475, packs against Loop 6, makes several hydrogen bonds and ionic interactions and further stabilizes the position of Loop 6. Conformational changes in these three regions lead to the complete occlusion of the active site. Although the C-terminal of Rubisco varies between different species, the interactions with Loop 6 are conserved. One of the highly conserved interactions involves Asp473, which has been proposed to be a latch site for keeping Loop six in a closed conformation (Duff *et al.*, 2000).

1.6 Mutagenesis studies

1.6.1 *Chlamydomonas reinhardtii* serves as a model system for the study of Rubisco

Mutagenesis of Rubisco in higher plants has been a challenging task for a number of reasons. The large subunit is encoded by the chloroplast *rbcL* gene (Chan & Wildman, 1972 Ellis, 1981) whereas the *rbcS* genes for the small subunit are located in nuclear genome (Kawashima & Wildman, 1972). Therefore the biosynthesis of Rubisco depends on the concerted interaction between the nuclear and chloroplast genetic systems and requires the aid of chaperones for folding and assembly. No eukaryotic Rubisco has been expressed successfully in any foreign host, most likely because of mismatches between the foreign Rubisco and the chaperone system of the host (Gutteridge & Gatenby, 1995).

Recently, it has been possible to transform and to specifically mutate the gene for the large subunit of Rubisco in plants (Whitney *et al.*, 1999). This led to the substitution of a leucine residue at position 335 by a valine. The recent advances make it possible to introduce point mutations in the Rubisco of higher plants to increase our knowledge of the structure/function relationship. However, Rubisco is a very large enzyme, with a molecular mass of about 560 kD. Therefore, it is

difficult to know precisely which residues influence the catalytic properties of the enzyme. In addition, because photosynthesis is essential for the survival of plants, if a mutation severely affects photosynthesis, the organism must be able to survive by other metabolic means.

The green unicellular alga *Chlamydomonas reinhardtii* is one of the most powerful model systems for exploring this enzyme for several reasons (Spreitzer, 1998). (1) Like green plants, *Chlamydomonas* Rubisco is a hexadecamer composed of eight large and eight small subunits. It has a sequence identity of approximately 90% in the large subunit with Rubisco of higher plants and the overall fold is very similar to that of Rubisco of higher plants (Taylor *et al.*, 2001). (2) *Chlamydomonas* can use acetate as an alternative source of carbon, a property that facilitates the isolation and maintenance of mutants inadequate in photosynthesis. (3) In *Chlamydomonas*, chlorophyll synthesis also occurs in the dark, therefore light is not essential for the assembly of photosynthetic apparatus, which makes it feasible to study light sensitive mutants. (4) The *rbcL* and *rbcS* genes of *Chlamydomonas* can be eliminated and/or replaced with mutant gene copies via genetic transformation of the chloroplast and nucleus, respectively.

Genetic screening and selection in *Chlamydomonas* has led to the recovery of several photosynthesis-deficient mutants. Some of these mutants have then been exploited for selecting second mutations that restore Rubisco function and photosynthesis.

1.6.2 The molecular basis for most mutants are still unexplored

To date there are more than 25 crystal structures of Rubisco deposited in the Protein Data Bank (PDB). These are structures of different forms of Rubisco (Form I, II, or III), activated or unactivated, complexed with different ligands or metal activators. From these structures together with genetic studies, it has been possible to identify several important structural features of the enzyme. These include the active site residues, Loop 6 region, and amino acids and regions at the interface between the large and small subunits.

Except for the active site residues, Loop 6 is perhaps the most intensively studied region of the enzyme. Genetic screening and selection in *Chlamydomonas* led to the discovery of a mutant of this flexible loop, V331A, which had a significant reduction in substrate specificity and V_c (Chen & Spreitzer, 1989). Later, two suppressor substitutions, T342I and G344S, were discovered that complemented the V331A substitution and restored the specificity factor to approximately wild-type level, (Chen *et al.*, 1993).

As described earlier, in the closed form of the enzyme, Loop 6 is stabilized by the interactions with the C-terminus of the large subunit, residues 467-475. A reduced carboxylase activity was observed upon removal of C-terminus of Rubisco from spinach or *Chlamydomonas* (Gutteridge *et al.*, 1993). The importance of this region, in particular residue Asp473, was further demonstrated by mutagenesis studies. Substitution of this residue with either an alanine or a glutamic acid

reduced catalytic efficiency of carboxylation and substrate specificity by 87% and 16% respectively (Satagopan & Spreitzer, 2004).

A second region that has been intensively studied is the region at the interface of the large and small subunits. Substitution of a leucine at position 290 at the bottom of β -strand 5 with an alanine in *Chlamydomonas* Rubisco causes decreases in V_c and substrate specificity, and an increase in the temperature sensitivity. The L290F mutant is a temperature conditional strain and grows at 25 °C, but lacks photosynthesis and requires acetate for growth at 35 °C (Chen *et al.*, 1993). Two suppressor mutations, A222T and V262L, were found that improved both the catalytic efficiency and thermal stability of L290F *in vivo* and *in vitro* (Hong & Spreitzer, 1997). Leu290, Ala222 and Val262 are situated far apart and far from the active site and they all interact with the β A- β B loop of the small subunit.

A region that shows large variation between species is the β A- β B loop of the small subunit (see section 1.5.3). To examine the significance of this loop, the *Synechococcus* β A- β B loop was replaced with the corresponding loop of the pea small subunit (Wasmann *et al.*, 1989). This chimeric *Synechococcus* small subunit was now able to assemble with pea large subunits. Within the β A- β B loop of the pea small subunit, a number of amino acid substitutions were created. The results showed that only substitution of Arg53 with a glutamate hindered holoenzyme assembly (Flachhmann & Bohnert, 1992). These studies indicate that the β A- β B loop may be important for assembly. Moreover, N54S and A57V small-subunit substitutions selected in *Chlamydomonas reinhardtii* acted as suppressor mutations that restored the decreases in V_c , thermal stability and specificity that resulted from an L290F mutation in the large subunit (Chen *et al.*, 1988, Du *et al.*, 2000). It is apparent that the β A- β B loop could be important for assembly, stability and specificity.

2. The aim of the thesis

An understanding of the structure-function relationships of a protein requires precise knowledge of the role of the residues (and regions) that are important for catalysis and stability of the enzyme. There is a natural variation in the catalytic efficiency of different Rubisco enzymes. It is worthwhile to put effort to establish the molecular basis for this disparity to further our knowledge of the nature of such relations.

Numerous mutational studies have been performed to investigate the regions and amino acid residues that influence the catalytic properties of the enzyme. Perhaps it is tempting to consider the active site residues the most obvious targets for improvement of Rubisco. A number of mutational studies in *R. rubrum*, *Synechococcus*, or *Chlamydomonas* Rubisco have shown that all the residues that interact with 2CABP are required for maximal rates of catalysis (Hartman *et al.*, 1994; Spreitzer, 1993). The analysis of structural changes within the active site upon any alteration of the enzyme is a crucial step, but since these residues are nearly 100% conserved among the large subunit of Rubisco from different species (Read & Tabita, 1994), and substitution of these cripple the enzyme, mutation of these residues are unlikely to improve the enzyme. The more promising approach for improving the efficiency of Rubisco is to investigate residues and regions that are farther from the active site. Obviously, we cannot improve the efficiency of such a large enzyme by a single mutation, and so far most of the mutations have led to an inferior enzyme. It is probable that improvement of Rubisco requires several changes simultaneously. Nevertheless, it is important to study even lethal mutations and investigate the structural alteration induced by these mutations to increase our knowledge of structure-function relationships. Many mutants have been selected and biochemically characterized, but the structural role of most of the mutated residues has not been determined. The aim of this thesis is to establish the structural role of some of these residues and regions. These include the role of the metal ion in the active site, Loop 6 residues and other residues in the vicinity of the active site, and residues and regions at the interface of the large and small subunits.

3. Methods

3.1 Cell growth, purification and crystallization

Chlamydomonas reinhardtii cell cultures were grown in the dark on an acetate medium at 28 °C (Spreitzer & Mets, 1981). Cells were harvested by centrifugation at 2500 g for 5 minutes and lysed by sonication in an extraction buffer consisting of 50 mM Bicine pH 8, 10 mM MgCl₂, 10 mM NaHCO₃, and 5 mM β-mercaptoethanol. A differential ammonium sulphate precipitation between 30 and 50 % saturation was carried out. The pellet was then dissolved in extraction buffer and loaded onto a Superdex-200 16/60 size exclusion column (Amersham Pharmacia). The fractions containing Rubisco were collected and loaded onto a MonoQ anion exchange column. Rubisco was eluted from the column with a 0.1-0.4 M NaCl gradient. The yield of the protein was 0.1-0.2 mg per litre of cell culture.

The photosynthesis-deficient, temperature-sensitive mutants of Rubisco from *Chlamydomonas reinhardtii* are difficult to grow in cultures to high density. This means that only minute amount of crystallization-grade protein can be purified. For the L290F mutant and the chimeric enzyme ABAN, it was necessary to grow over 10 litres of cell culture to obtain sufficient amount of crystallization quality protein.

Purified protein was concentrated to a final concentration of 10 mg/ml in an activating buffer containing 50 mM HEPES pH 7.5, 10 mM NaHCO₃, and 5 mM MgCl₂. Crystals of the Rubisco mutants were grown using the hanging drop vapor diffusion method at 20 °C by mixing a drop (3-4 µl) containing equal amounts of the protein sample in activating buffer containing 1 mM 2-carboxy-D-arabinitol 1,5-bisphosphate (2CABP) and a well solution consisting of 50 mM HEPES pH 7.5, 0.05-0.2 M NaCl, 7-12% PEG 4000, 10 mM NaHCO₃ and 5 mM MgCl₂. Crystals usually appeared within one week.

3.2 X-ray crystallography

Scattering is a phenomenon, which occurs when an electromagnetic wave interacts with an obstacle. From analysis of the nature of the scattering, we can obtain information about the structure of the obstacle. X-rays are electromagnetic radiation with a wavelength between 0.1-10 Å. Since this is comparable to the distances between bonded atoms within molecules, we use X-ray diffraction to determine the structure of molecules.

A crystal (of *e.g.* a protein in this case) has a well-defined, long-range, three-dimensional molecular order because it arranges huge numbers of molecules in the same orientation, so that the scattered waves in the same direction add up and give a detectable signal. In a crystal, the diffracting power is inversely related to the size of the molecules in the crystal. Protein molecules are large, therefore their

crystals diffract X-rays much weaker than the crystal of smaller molecules. This problem is pronounced for the crystals of Rubisco. Rubisco is very large, which results in crystals with large unit cells. There is therefore an absolute need for synchrotron radiation as the X-ray source to obtain even medium-resolution data of Rubisco. Obtaining high-resolution data of Rubisco crystals requires synchrotron radiation of high intensity and low divergence.

Synchrotron radiation is extremely intense, this allows faster data collection, which in turn reduces time-dependent radiation damage of the crystal. It is also highly collimated, as a result the X-ray beam is less divergent. A problem with data from crystals with large unit cells such as Rubisco is that the diffraction peaks are very close together and often difficult to resolve. This problem is less severe with synchrotron radiation because the X-ray beam is highly parallel.

3.3 Molecular replacement

Once diffraction data have been collected, we need to determine the phases. Unfortunately, the diffraction data do not contain the necessary information on the phase angles. If the structure of a homologous protein or the same protein from a different crystal form is known, the structure can be determined by the method of molecular replacement (Rossmann & Blow, 1960). In this method, the phases of the known structure are used as the first approximate start phases for the unknown structure. Thus the problem is reduced to the transfer of the known protein structure to the crystal of the protein for which the structure is not known. Placement of the known structure, the search molecule, in the target unit cell consists of two steps: (i) determination of the orientation of the molecule within the cell (rotation) (ii) determination of the position of the correctly oriented molecule within the same cell (translation). Rotation consists of overlapping the interatomic vectors (Patterson vectors) of the search structure with those of the unknown structure in three dimensions. Translation consists of determining the translation required to overlap the search molecule with the target molecule in real space. The solution obtained serves as a first approximate model that can subsequently be refined.

The success and quality of the solution of molecular replacement depends highly on the quality and completeness of the diffraction data and on the similarity between the structure of the search model and that of the target protein. For refinement of the newly determined structure, the resolution at which the structure of the search model has been determined can be of great importance. The availability of high resolution structures for both spinach Rubisco, 8RUC (Andersson, 1996) 1.6 Å and *Chlamydomonas reinhardtii* Rubisco 1GK8 (Taylor *et al.*, 2001) 1.4 Å has had a major contribution on the quality of the structures that will be discussed throughout this thesis. In each case, crystallographic measures of quality including R factors and electron density maps were excellent, largely reflecting the high resolution of the starting model in and the completeness of the data.

3.4 Non-crystallographic symmetry

Rubisco is a hexadecamer of eight identical large (L) and small (S) subunits. The entire molecule displays 422 symmetry and this often results in non-crystallographic symmetry (NCS). Within the crystal NCS arises when there is more than one molecule in the asymmetric unit (or as in this case more than one identical subunit). The relative positions of the molecules can be determined and used for map improvement (averaging) and improvement of statistics in refinement. In Rubisco, the molecular symmetry allows for up to 8-fold NCS constraints/restraints per molecule in the asymmetric unit. The diffracting power of a protein crystal is inversely related to the size of its building blocks, the unit cells. Rubisco is a large molecule, therefore the unit cell volume of Rubisco crystals is usually large, leading to weakly diffracting crystals. The use of NCS restraints in refinement considerably improved the observation to parameter ratio in refinement and resulted in greatly improved electron density maps. This allowed detailed conclusions to be drawn even from single-site mutants.

3.5 Temperature factors

Structure determination by X-ray crystallography does not deal with a single molecule at an instantaneous point of time. A crystal is an ensemble of many millions of molecules that are packed in an orderly manner. Because molecules and atoms undergo thermal fluctuations, they can adopt different conformations with respect to time and/or space. Therefore the crystal structure does not give the exact position of each atom but rather a probability function, representing the time-space averaged electron density around a central mean position. The temperature factor of an atom is a quantity that relates the mean displacement of the particular atom from its mean position. Two common sources that may give rise to overall mean displacement of an atom are internal static disorder and internal dynamic disorder. The first is a result of different conformations in different unit cells whereas dynamic disorder occurs as a result of vibration within molecules and is temperature dependent. However the contribution of dynamic disorder can not be quantified, unless intensity data are collected at different temperatures (Drenth, 1994; Parak, 1989).

Analysis of temperature factors delivers information about which atoms in the molecule have the most freedom of the movement. High temperature factors of certain regions of a refined structure often indicate that those regions are more disordered.

3.6 Merohedral twinning

Twinning is a crystal growth anomaly in which the crystal is composed of distinct domains with different orientations. Two basic types of twinning may be identified: epitaxial twinning, in which the lattices from the individual repeating units overlap in one or two dimensions, and merohedral twinning, when the lattices of the different domains overlap in three dimensions (reviewed in Yeats, 1997). Merohedral twinning results in observed diffraction spots, which do not represent individual intensities but contain contributions from two or more twin-

related reflections. Twinning usually prevents a successful structure determination unless it is detected and either avoided or corrected. The most common type of merohedral twinning involves only two different domains, which is called hemihedral twinning. If the symmetry operation relating the different twin domains can be determined, the data can be detwinned, but this amplifies experimental errors.

In the $C222_1$ crystals of Rubisco, the packing results in similar lengths of the a- and the b-axes (155.88 Å, 156.25 Å) of the unit cell (Andersson & Brändén, 1984). This gives rise to the possibility of pseudo-merohedral twinning. In the past, structures of the spinach enzyme could be solved by carefully avoiding the merohedrally twinned crystals by elaborate screening (Andersson & Brändén, 1984; Andersson et al., 1989; Knight et al., 1990; Taylor & Andersson, 1997).

To investigate the differences between the calcium and magnesium ion in Rubisco, two crystal forms of Rubisco complexed with Ca^{2+} and the transition state analogue 2CABP were obtained. One was prepared by co-crystallizing 2CABP with Rubisco/ Ca^{2+} complex and the second one by soaking 2CABP into preformed crystals of Rubisco/ Ca^{2+} -3PGA. The co-crystallized crystals belong to the space group $P2_12_12$ and the soaked crystals belong to the space group $C222_1$. Analysis of the intensity distribution revealed that the latter crystal was merohedrally twinned. Furthermore, screening of a large number of crystals indicated that the twinning problem was much more severe in this case, occurring in almost every crystal used.

Refinement of the structure against the twinned data resulted in high R-factors. To improve the refinement statistics, the data were detwinned and the structure was refined against the detwinned data. This reduced the R-factors slightly, but worsened the quality of the electron density maps because of the errors introduced by detwinning. The structures of Rubisco- Ca^{2+} /2CABP obtained from the two different crystals ($P2_12_12$ and $C222_1$) are very similar.

4. Results and discussion

4.1 The active site and the role of the metal ion

The structures of hexadecameric Rubisco in the Protein Data Base occur in two distinct forms, the open form where the active site is open to the bulk solvent, and the closed form in which the flexible elements are ordered. The ordering results in the complete occlusion of the active site (Taylor & Andersson, 1996). The structure of Rubisco from spinach complexed with its natural substrate RuBP was determined with Ca^{2+} instead of Mg^{2+} as the activating metal ion (Taylor & Andersson, 1997). This structure is open with Loop 6 partially ordered. This observation raised several questions: does the different nature of calcium compared to magnesium prevent loop closure upon RuBP binding? Why does Ca^{2+} not sustain catalysis? Is it possible that this ion is not able to trigger loop closure and turnover in the same way as Mg^{2+} due to the difference in atomic properties of calcium? To address these questions we determined the structure of Rubisco complexed with Ca^{2+} and 2CABP, a ligand known to support closed complexes. This was done by cocrystallisation and by soaking of 2CABP into crystals of the open form with the weaker ligand 3PGA.

Both structures resemble the closed Mg^{2+} -2CABP complex. Loop 6 is ordered over the active site and calcium is bound to six oxygen ligands, three of which are provided by 2CABP and the other by Asp203, Glu204 and the carbamate of Lys201.

Calcium has a significantly larger ionic radius (0.95 Å) than magnesium (0.6 Å). This has consequences for the role that these ions play in biology (see Paper I):

1. Lengthening of certain bond distances in the Ca^{2+} complex. A closer analysis of the distances in the active site region shows that the distance between the C3 carbon of the substrate and the oxygen of the carbamate has increased from 3.3 Å to 3.5 Å (Table 4.1). The carbamate has been implicated in the enolisation step, proton abstraction from the C3 of RuBP (Taylor & Andersson, 1997). The increase in the bond distance may impede the process of the proton hop thereby hampering formation of the RuBP enediolate.
2. The charge density on Ca^{2+} is lower than on Mg^{2+} . This makes Ca^{2+} less polarizing *i.e.* a weaker Lewis acid than Mg^{2+} , which may affect the stability of the electronic transition to form the enediol.
3. Like Mg^{2+} , Ca^{2+} can also bind six ligands, however Ca^{2+} often has an irregular flexible coordination sphere with coordination number of 6-8 whereas Mg^{2+} has a regular rigid coordination sphere with a coordination number of exactly six (Harding, 1999). As a result, the coordination around Ca^{2+} is a distorted octahedron. In the case of Rubisco, this in turn has influenced the degree of the curvature of 2CABP and the distance between the two phosphate binding sites, P1

and P2, has increased from 8.9 Å in the Mg²⁺-2CABP complex to 9.1 Å in the Ca²⁺-2CABP complex.

4. The rate of ligand exchange is different for Ca²⁺ and Mg²⁺. This may influence the dynamics of the reaction.

Table 4.1. Distances of the activator metal ion to 2CABP and to some residues in the active site. The distances show clearly that the coordination sphere is larger in the structure of Ca²⁺-2CABP-Rubisco complex than the corresponding Mg²⁺ complex.

Atom	Ca ²⁺ complex (Å)	Mg ²⁺ complex (Å)
Mg ²⁺ -2CABP O2	2.7	2.4
Mg ²⁺ -2CABP O2	2.8	2.4
Mg ²⁺ -2CABP O2	2.7	2.3
Mg ²⁺ -E204 OE1	2.5	2.3
Mg ²⁺ -D203 OD1	2.7	2.2
Mg ²⁺ -K201 OX2	2.7	2.3
2CABP C3-K201 OX1	3.5	3.3
2CABP P1-2CABP P2	9.1	8.9

4.2 The redox state of cysteine 172 influences Rubisco's activity and susceptibility to degradation

Although the regulation of Rubisco has been studied extensively (Salvucci & Ogren, 1996) redox regulation has obtained less attention. Studies have indicated that oxidation of some cysteine residues may influence the activity and the susceptibility to proteolysis of the enzyme (Garcia & Moreno, 1993). The number of cysteine residues in the large subunit of Rubisco from different species varies. Rubisco from *Clamydomonas* and spinach have 9, but the enzyme from *Ralstonia eutropha* has 6. Among higher plants, Cys172 is the most strictly conserved cysteine. This residue is situated in the vicinity of the active site and adjacent to another cysteine at position 192.

4.2.1 Substitution of Cys172 by serine increases the CO₂/O₂ specificity

To elucidate the functional role of the two cysteines, C172S and C192S mutants were produced. Analysis showed that both mutants had significant alterations in their catalytic properties and thermostability (Paper IV). It was also shown that as a result of these alterations, the C172S mutant had about 12% increase in substrate specificity compared to the wild-type, while the specificity factor of C192S mutant was identical to wild-type.

4.2.2 Structural changes induced by the C172S substitution

Superposition of the C172S, C192S and wild-type structures shows no dramatic differences in the overall structures. However, a closer inspection reveals that the main chain of residues 170 to 174 is displaced about 0.4 Å in the structure of C172S compared to wild-type (Figure 4.1) High resolution crystal structures of

Chlamydomonas Rubisco (Taylor *et al.*, 2001) and spinach Rubisco (Andersson, 1996) show that Cys172 and Cys192 are only in van der Waals distance and they are not engaged in disulfide bonding. In the high resolution structures, Cys172 and Cys192 are too far apart (3.9 Å) and with a wrong orientation to be able to form a disulfide bond. Cys172 interacts with the phosphate-binding residue Phe402 and is close to residues Thr173 and Lys175 that interact with the substrate. Formation of a disulfide bond between Cys172 and Cys192 would require a significant shift of the backbone atoms of strand 1, or helix 1, or both. Due to the critical position of C172, this shift may have deleterious effect on the active site geometry. These findings suggest that a disulfide bridge between Cys172 and Cys192 may act as a dynamic molecular switch that could activate or deactivate Rubisco. This study shows replacement of Cys172 by serine affects thermosensitivity and the catalytic properties of the enzyme and also modifies the structure. Because similar changes are not observed in C192S mutant, it appears that Cys172 residue is an essential residue for the structure and catalytic efficiency of Rubisco.

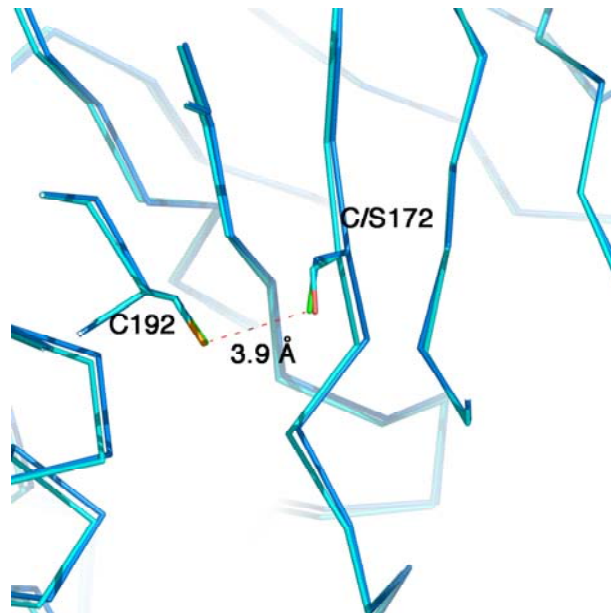


Figure 4.1 Superposition of the wild-type *Chlamydomonas* and the C172S mutant structures. *Chlamydomonas* is shown in blue and C172S mutant is depicted in cyan.

4.3 Elements involved in the dynamics of catalysis

The loops connecting secondary structure elements are generally less conserved and more mobile than the secondary structure elements that they connect. However, they are therefore not of less interest, since in many cases they are involved in catalysis or binding of the substrate. In this case they may be highly conserved (Eric *et al.*, 1993).

4.3.1 Mutation at the base of Loop 6 influences the CO₂/O₂ specificity

In Rubisco, the flexible Loop 6 (residues 331-338), which is positioned at the top of the eight-stranded α/β -barrel, plays a crucial role in binding of the gaseous substrate and thereby influences catalysis of both carboxylation and oxygenation. There are some variations in the amino acid sequence of Loop 6 between different species, but most of these residues are highly conserved among Rubisco of higher plants and green algae. Mutational studies have shown that replacement of Val331 situated at the N-terminal end of this loop with an alanine has a detrimental effect on the activity of the enzyme. A second mutation, in which Thr342 was replaced with an isoleucine, restored the activity to more or less wild-type level (Chen & Spreitzer, 1989).

Val331 is situated in a hydrophobic pocket and makes van der Waals interactions with Thr342, Ile393, Gly337 and Arg339 (Taylor *et al.*, 2001). The structure of V331A shows that the introduction of the less bulky side-chain of alanine results in loss of most of these interactions. In the structure of the suppressor double mutant, the introduction of isoleucine in place of threonine at position 342 has compensated for most of these losses (see Paper V for details of the interactions). The replacement of Val331 by alanine has also caused disorder in the C-terminus of the large subunit and as a result no density was observed for the last residue, Leu475.

4.3.2 Importance of the C-terminus

Although it is not clear from the structure how this substitution may induce disorder in the C-terminus of the large subunit, it has been suggested that the C-terminus of the large subunit has a crucial function in the stability of Loop six (Knight *et al.*, 1990), thus disorder in this region may influence the catalytic ability of the enzyme. Asp473, a highly conserved residue of the C-terminus has been proposed to function as a latch residue that holds Loop 6 over the active site in the closed form (Duff *et al.*, 2000). The replacement of Asp473 with an alanine or a glutamate caused more than 85% decrease in carboxylation efficiency of the enzyme (Satagopan & Spreitzer, 2004). In the structure of wild-type *Chlamydomonas* Rubisco, the back-bone amide of Asp473 hydrogen bonds with Arg336 and the side chain makes ionic bonds with His310 and Arg134 (Figure 4.2). Presumably, the larger side-chain of glutamate in place of aspartate cannot be accommodated, causing disorder of C-terminus (residues 469-475). The structure of the mutants indicate that the stability of Loop 6 over the active site is maintained by the interactions between Loop 6 with the active site as well as with the C-terminus of the large subunit. It is interesting to note that structural-based sequence alignment shows that in Rubisco from *Ralstonia eutropha* residue 331 is an alanine and residue 342 is a valine.

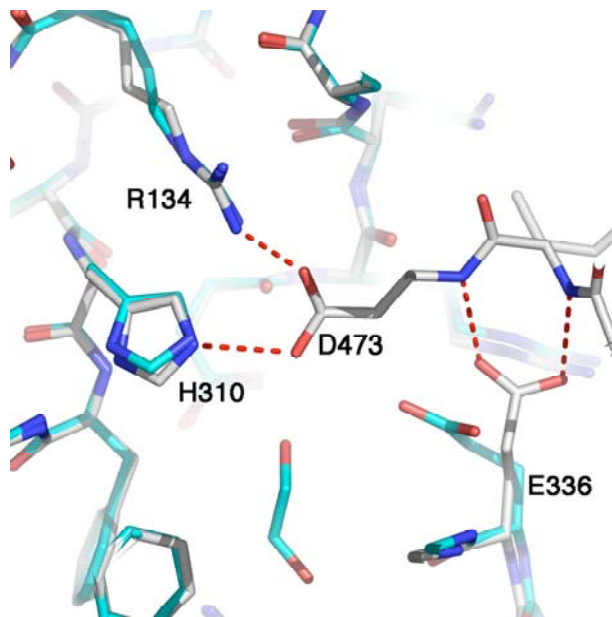


Figure 4.2 Superposition of *Chlamydomonas* wild-type and D473E mutant structures. *Chlamydomonas* is shown in gray and the mutant enzyme is depicted in cyan. Asp473 makes hydrogen bonds with Arg134 and His310. It also makes hydrogen bonds with Glu338 of Loop6. In the structure of D473E mutant, residue 473 is disordered and as a result all the interactions are lost.

4.4 Interactions at the interface of small and large subunits influence stability and catalytic ability of Rubisco (paper II and III)

4.4.1 Leucine 290, a critical residue at the interface of large and small subunits

The holoenzyme of Rubisco from land plants and green algae is composed of eight large and eight small subunits. Although much is known about the structure-function relationship of the chloroplast-encoded large subunit and the active site geometry is well understood from a variety of structural studies, much less is known about the nuclear-encoded small subunit.

Form II Rubisco is composed of large subunits only, which indicates that small subunits are not absolutely necessary for the activity of the enzyme. However, the kinetic parameters of this enzyme are too poor to sustain photosynthetic growth in the presence of oxygen. Furthermore, in the absence of the small subunits, Form I Rubisco has almost no carboxylase activity (Andrews, 1988). In addition, there is a significant difference in the catalytic efficiency and specificity between the Form I and Form II enzymes. Hence it is clear that the kinetic behaviour of the enzyme is influenced by long range interactions provided by the small subunit. These facts

raise a few questions. What is the role of the small subunit? Is it possible to use the small subunit as a route for engineering a more efficient Rubisco?

Mutant screening and selection in *Chlamydomonas reinhardtii* identified a L290F substitution that had a (13%) reduction in substrate specificity (Chen *et al.*, 1988). Further investigation revealed that this mutant has a reduced thermal stability (Chen *et al.*, 1993). *Chlamydomonas* cells containing this mutation could grow autotrophically at 25 °C, but not at 35 °C. Two suppressor mutations, A222T and V262L, were recovered that restored photosynthesis of the L290F mutant more or less back to the wild-type level at the restrictive temperature (Hong & Spreitzer, 1997). The double mutants L290F/A222T and L290F/V262L had improved thermal stability and specificity. To understand the structural role of Leu290 and Ala222, the structures of L290F and L290F/A222T Rubisco mutants were solved.

Residue 290 is situated at the beginning of β -strand 5 of the carboxy-terminal α/β -barrel domain of the large subunit, far away from the active site (distance from the C α atom to the magnesium ion at the active site is ~ 18 Å). Residue 222 is situated in the middle of α -helix 2, also far from the active site (distance from the C α atom to the magnesium ion at the active site is ~ 20 Å). Thus, it is obvious that the effect of substitution of these residues on the catalytic properties of the enzyme must be indirect. Moreover, an inspection of the structures of the L290F and L290F/A222T mutants shows that the structures are almost intact compared to the structure of the wild-type enzyme. The substitution of leucine by a phenylalanine in the structures of the single and double mutant Rubisco has caused small shifts of the side-chains of Lys161 and Val262 of the large subunit and Leu66 of the small subunit. Most likely, these changes cannot solely explain why these substitutions have such large impacts on the catalytic properties of the enzyme. The question arises, if these substitutions do not cause significant perturbations of the structure, how are the changes transmitted to the active site? Analysis of the temperature factors suggests that the changes influence the dynamics of the enzyme without gross structural changes.

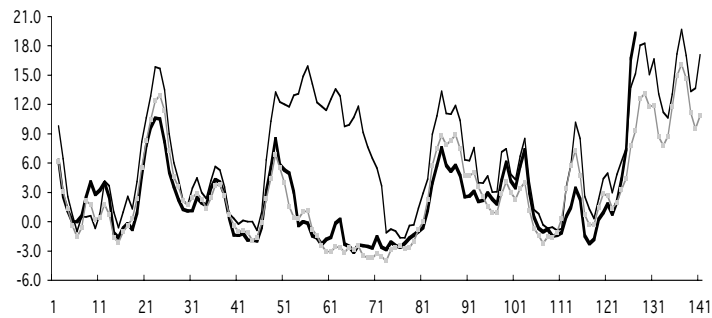
4.4.2 Temperature factors contain valuable information on the dynamics of the enzyme

Analysis of the temperature factors reveals considerable differences between the L290F mutant and both the L290F/A222T mutant and the wild-type enzyme (Figure 4.3). Each atom in a crystal structure has a temperature factor (B-factor) associated with it, which shows the degree of thermal motion of that atom. The B-factor is a measure of disorder of that atom and generally flexible loops and regions that are not buried have higher B-factors. Residues 290 and 222 are situated at the interface of the large and small subunits. Analysis of the crystal structures reveals that these residues are connected via long-range interactions. Although these residues do not interact with each other directly, they both make interactions with the intervening residues Val262 and Pro263 of the loop connecting α -helix 3 and β -strand 4 within the same large subunit. A second set of interactions between them is *via* Cys65, Leu66 and Tyr67 of the small subunit

(see Paper II for details of the interactions). Leu66 and Tyr67 are positioned in a hairpin loop (the β A- β B loop, residues 45-72) connecting strands A and B of the small subunit. In the structure of the single mutant, the entire hairpin loop (residues 50-72) and residues 161-164 and 259-264 of the large subunit exhibit elevated temperature factors compared to the wild-type enzyme. In contrast, no obvious increase of the B-factors was detected in the double mutant.

The higher temperature factors in the structure of the single mutant Rubisco could explain the decreased levels of Rubisco in L290F cells grown at restrictive temperatures (35 °C) relative to the amount of holoenzyme in L290F/A222T revertant cells. The single mutant displays increased thermal motion in the regions concentrated around the mutation site and is thermally unstable. The second substitution restores the temperature factors to the wild-type level and improves the catalytic efficiency and the thermal stability of the enzyme.

a



b

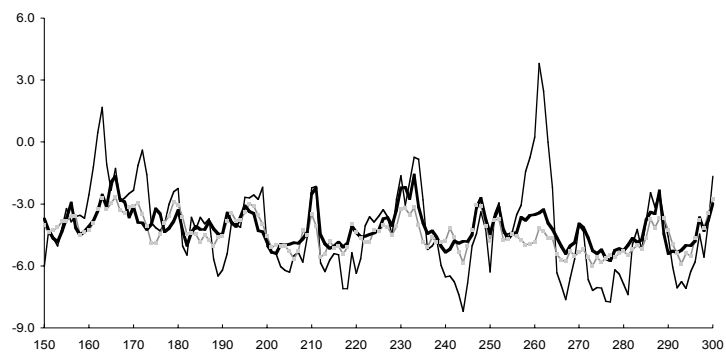


Figure 4.3 Atomic temperature factors (B factors) corrected for crystal disorder. (a) Large subunit, (b) small subunit. L290F, thin black line; L290F/A222T, thin grey line; wild-type, thick black line.

4.4.3 Disorder may be transmitted to the active site via long range interactions

The structure of the active site of L290F is indistinguishable from those of the L290F/A222T and the wild-type enzyme. The active site is far from both the mutation sites. How could the effect of these mutations be transmitted to the active site?

Residue 290 is situated at the N-terminus of strand 5, only 4 residues away from His294 (Figure 4.4) At the C-terminal side of strand 5, residue His294 is in hydrogen-bonding distance to 2CABP as well as carbamylated Lys201 and Glu204 of the active site. It is conceivable that the single mutation may influence the dynamics of the protein, and these changes could be transmitted to the active site *via* such long-range interactions.

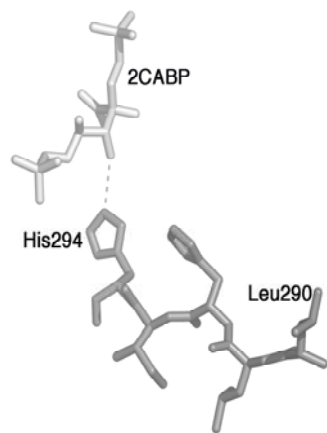


Figure 4.4 Leu290 is positioned at the N-terminus of the active site, only four residues away from His294 in the active site.

A second long-range interaction through which the active site could be influenced is *via* Glu158. This residue is situated in a hydrophobic cleft lined by leucine residues Leu162, Leu169 and Leu290. There is a network of hydrogen bonds that extends from Glu158 through His325 and His292, terminating at His327. His327 is situated in the active site and interacts with 2CABP (Figure 4.5).

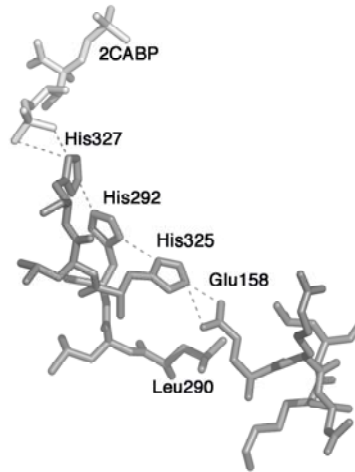


Figure 4.5 The side chain of Leu290 packs against Glu158. There is a network of hydrogen bonds that extends from Glu158 to 2CABP at the active site.

4.4.4 The β A- β B loop makes a major contribution to the stability of the enzyme

The small subunits are generally more divergent than the large subunits and there is great variation in the number of residues within the small subunits from different species. Therefore it is reasonable to assume that the small subunits make some contribution to the differences in the efficiency of the enzyme from different species. It is interesting to note that the detrimental effect of the single mutation, L290F, is reflected on a region of the small subunit (β A- β B loop), which varies considerably in diverse species. For example in the small subunit of prokaryotic and non-green algae, this loop is ten residues shorter than that of green plants whereas the corresponding loop of *Chlamydomonas* Rubisco is five residues longer. Although the small subunit is less conserved than the large subunit, some small-subunit interactions are highly conserved in Rubisco from higher plants and *Chlamydomonas*. Such interactions are, for instance, the interactions made by Arg71 (Arg65 in spinach) situated at the C-terminal end of the β A- β B loop.

To elucidate the importance of this loop for catalytic efficiency and holoenzyme stability, the β A- β B loop of *Chlamydomonas* Rubisco was replaced with the corresponding loops of the cyanobacterial (ABAN) and spinach (ABSO) Rubisco. Insertion of the cyanobacterial or spinach loop in *Chlamydomonas* Rubisco did not prevent holoenzyme assembly. However, biochemical analysis showed that the amount of holoenzyme of mutant ABAN was less when cells were grown at 35 °C. It also became apparent that ABAN had reduced carboxylase efficiency at the elevated temperature. ABAN had no activity after 10 minutes at 60 °C, whereas ABSO had almost half of its activity after incubation at the same temperature. Whereas the substrate specificity of ABSO was almost identical to that of the wild-type, an 11% decrease was observed for the ABAN enzyme.

The structures of ABAN and ABSO show that the β A- β B loops have similar conformations as the corresponding loops of Rubisco from *Synechococcus* and spinach. The active sites of the two chimeric enzymes are virtually intact, except

for small changes in the distances of some active-site amino acids to 2CABP (Table 4.1). This suggests that the effect of replacing the loop of *Chlamydomonas* Rubisco on the stability and catalytic properties of the enzyme must be indirect, similar to the L290F mutation.

Table 4.1 Distances between residues in the active site and the transition state analogue 2CABP in the structures of wild-type *Chlamydomonas* Rubisco and the chimeric constructs ABSO and ABAN.

Residue-2CABP	wild-type	ABSO	ABAN
Thr65 OG1-O1P	2.66	2.59	2.42
Thr173 OG1-O2	2.79	2.97	2.89
Arg295 NE-O6P	2.87	2.76	2.68
Arg295 NH2-O4P	2.83	3.02	2.79
His327 ND1-O5P	2.70	2.93	2.77
Lys334 NZ-O7	2.93	2.63	2.83
Lys334 NZ-O3P	2.81	2.47	2.85
Ser379 OG-O4	2.91	3.32	2.80
Ser379 O-O4	2.98	3.28	2.90
Gly404 N-O1P	2.74	2.66	2.96

Although the β A– β B loop is one of the more variable regions of Rubisco from different species, there are four residues within the loop (Tyr67, Tyr68, Asp69 and Arg71) that are highly conserved among Rubisco from green algae and land plants. Substitution of these residues by alanine showed that only the mutant R71A had a reduced thermal stability (Spreizer *et al.*, 2001).

4.4.5 Comparison of the structures of ABAN, ABSO and wild-type *Chlamydomonas* Rubisco

Because of the shorter β A– β B loops of ABSO and ABAN, there are major alterations in the interactions provided by these loops compared to the wild-type *Chlamydomonas* enzyme. Structure-based alignment (Figure 4.6) shows that in place of Glu46 in the beginning of the loop in the wild-type *Chlamydomonas* and ABAN enzymes, there is a threonine in ABSO. This residue makes van der Waals interactions with Phe94 of the same small subunit and Val7 of the neighboring small subunit. The same interactions provided by this threonine are present in the structure of spinach Rubisco. In contrast, because the side-chain of Glu46 is further away from Phe94 and Ala7 in the ABAN and wild-type *Chlamydomonas* Rubisco, these interactions are absent. In wild-type *Chlamydomonas*, the side chain of Ser56 packs against the side-chain of Tyr226 of the large subunit. The hydroxyl group of Tyr226 is involved in a number of hydrogen bonds. The shorter loop of ABAN allows the side-chain of Tyr226 to swing out towards the solvent channel and as a result all the interactions are lost.

	45	46	47	48	49	50	51	52	53	54	55	56	57	58
WT	A	E	A	D	K	A*	Y*	V*	S	N	E	S	A	I
ABSO	A	T	D	H	---	G	F*	V*	Y	R	E	H	H	N
ABAN	A	E	H	---	---	S	N*	P	E	---	---	---	---	---

	59	60	61	62	63	64	65	66	67	68	69	70	71	72
WT	R	F	G	S	V	S	C	L	Y	Y	D	N	R	Y
ABSO	---	---	---	---	---	S	P	G	Y	Y	D	G	R	Y
ABAN	---	---	---	---	---	---	---	---	---	---	---	E*	F*	Y

Figure 4.6 Structure-based alignment of the β A- β B loop of wild-type *Chlamydomonas* Rubisco, ABSO and ABAN. The loop of *Chlamydomonas* Rubisco starts at Glu46 and ends at Arg71.

* Not in perfect alignment

--- Residue missing at this position

4.4.6 Interactions at the subunit interface influences the thermal stability of Rubisco

The surface area buried between the β A- β B loop and the neighboring subunits was calculated for the chimeric enzymes and their corresponding wild-type enzymes from spinach and *Synechococcus* (Paper III, Table 3). The results show that the surface area buried in ABAN is reduced by 21% relative to that in *Synechococcus* Rubisco whereas the surface area lost in ABSO compared with the spinach enzyme is only about 3% (Figure 4.7). The total interaction area of the β A- β B loop in ABSO is similar to that of spinach Rubisco whereas in ABAN a significant interaction area is lost compared to the *Synechococcus* enzyme because the context of the *Chlamydomonas* enzyme cannot compensate for contacts lost to the loop. The loss of interactions at the subunit interface may explain the temperature sensitivity of ABAN.

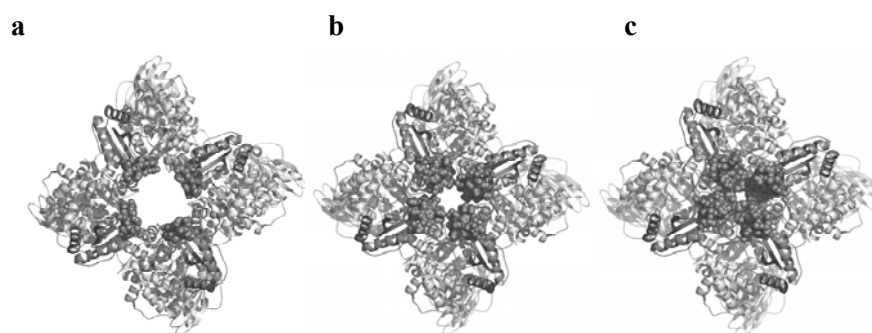


Figure 4.7 The β A- β B loop of (a) ABAN (b) ABSO and (c) wild-type *Chlamydomonas* Rubisco. The large subunits are shown in gray, the small subunits are illustrated in black and the β A- β B loop is depicted as black spheres.

4.4.7 Arg59 and Arg71 are critical residues at the interface of large and small subunits

Superposition of the structures of wild-type *Chlamydomonas* Rubisco and ABSO shows that whereas the back-bone of Asn54 of *Chlamydomonas* Rubisco is in the place of an arginine (Arg53 in spinach and ABSO), the guanidino group of Arg59 from a neighboring small subunit of the *Chlamydomonas* enzyme is in perfect alignment with the guanidino group of Arg53 of ABSO. The guanidino group of this arginine (Arg59 of *Chlamydomonas* Rubisco or Arg53 of ABSO) makes hydrogen bonds with Tyr226 and Gly261 of the large subunit and Ser64 within the same small subunit (Figure 4.8).

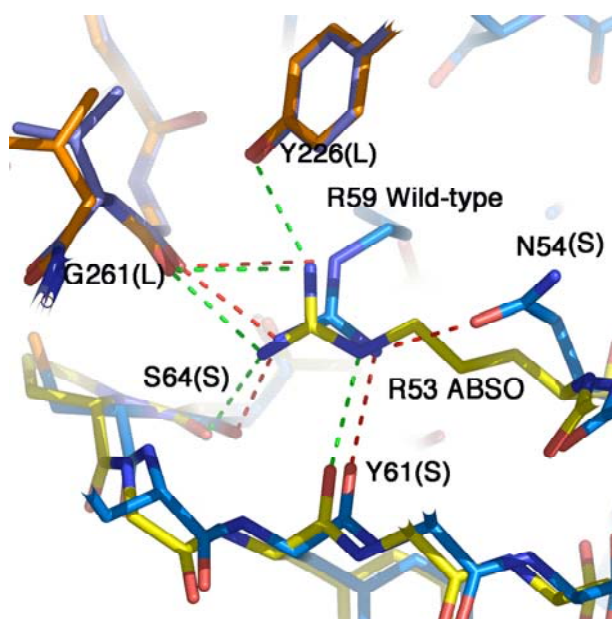


Figure 4.8 Superposition of the structures of wild-type *Chlamydomonas* Rubisco and the chimeric enzyme ABSO. *Chlamydomonas* Rubisco is shown in blue (L) and cyan (S) and ABSO is illustrated in yellow (S) and orange (L). The side chain of ARG59 of the wild-type *Chlamydomonas* enzyme makes several hydrogen bonds with large and small subunits. In ABSO, the side chain of Arg53 of the neighbouring large subunit is in place of the side chain of Arg59 in the wild-type and it makes similar hydrogen bonds.

A similar set of interactions is provided by Arg71 (Arg65 in ABSO and spinach Rubisco) situated at the C-terminus of the β A- β B loop. Arg71 makes hydrogen bonds with Lys161 of the large subunit and Glu223 of the neighboring large subunit and the methylene groups of Arg71 make packing interactions with Lys161. While almost identical interactions are present in ABSO and spinach Rubisco, because of the shorter loop, these interactions are missing in ABAN (Figure 4.9).

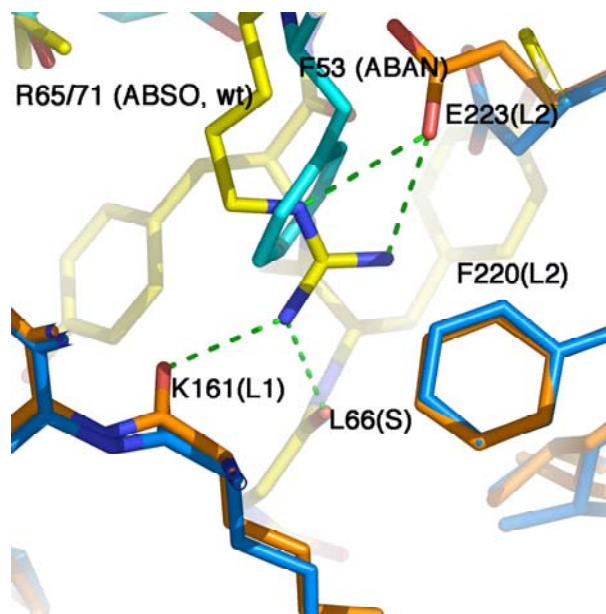


Figure 4.9 Superposition of the structures of the chimeric enzymes ABSO and ABAN. ABSO is shown in yellow (S) and orange (L) and ABAN is depicted in cyan (S) and blue (L). Arg65 of ABSO (Arg71 in wild-type *Chlamydomonas*) makes one hydrogen bond with Lys161 of the large subunit (L1) and two hydrogen bonds with Glu223 of the neighbouring large subunit (L2). In ABAN Phe53 has replaced Arg65 and all the hydrogen bonds are lost.

Because of its capacity for making multiple types of interaction, arginine is one of the most common amino acids at protein-protein interfaces (Bogan & Thorn, 1998). The three methylene carbon atoms give arginine a hydrophobic character while it is also capable of making several hydrogen bonds with its positively charged guanidinium group. This is the case with Arg59 and Arg71. They are positioned at the C- and N-terminus of the β A- β B loop and may function as bolts holding the subunits together. Lack of these arginines may make major contributions to thermal instability of ABAN.

5. Future perspectives

This thesis has pinpointed some of the areas and residues that influence the CO₂/O₂ specificity. However, with one exception all substitutions studied here led to a negative change of the specificity. In order to arrive at a list of the “best” substitutions for engineering a better Rubisco, one would need to use a broader approach and study groups of changes using *e.g.* combinatorial techniques rather than a single-site substitution. It seems like every investigation at the field of Rubisco raises a number of questions.

This work has shown that the closure of Loop 6 is not hindered by calcium and it is feasible to induce loop closure by the soaking of this ligand into crystals of carbamylated enzyme in complex with Ca²⁺. However, we can still make only an educated guess of the reasons for the inability of Ca²⁺ to sustain catalysis. Given rubisco is a very slow enzyme, would it be possible to flash-freeze a complex of Mg²⁺-activated Rubisco with RuBP and obtain a dataset of the substrate complex or some early intermediate? Would it be possible to find an analogue of the enediolate? D-glucose-2,3-pentodiulose-1,5-bisphosphate is a slow and tight-binding inhibitor of Rubisco (Kane *et al.*, 1998). If this could be produced in stable and sufficient amounts, it might be possible to grow crystals in an anaerobic environment.

It has been suggested that the redox state of Cys172 plays a role in regulation of the activity of Rubisco. The structure of the C172S mutant shows that the backbone of residues 170 to 174 of the large subunit has shifted about 0.4 Å. What would the structure look like if we could capture Cys172 in an oxidized state? This would require a different strategy for data collection to avoid reduction by the X-ray beam (Berglund *et al.*, 2002). The structures of wild type Rubisco from different species show that Cys172 and Cys192 are not engaged in disulfide bonding. Disulfide bonding will require a significant shift of the backbone atoms of strand 1, or helix 1, or both, which could have significant impact on the active site geometry.

A puzzling feature of Rubisco is the presence of the small subunit. Rubisco with only a dimer of large subunits, Form II Rubisco, is a competent catalyst, but the presence of small subunits enhances the catalytic efficiency tremendously. Small subunits are more divergent than large subunits and there has been a correlation observed between the variation in the small subunits and variation in the catalytic efficiency of Rubisco from different species. What is the role of the small subunit? Sequence alignments show that the most conserved residues of small subunits are the ones that are in contact with the large subunits. Structures of the L290F mutant and the chimeric enzymes ABAN and ABSO highlight the importance of the small subunits for the stability of the holoenzyme. The structures of ABAN and ABSO show that the βA–βB loop plays a significant role in the stability and thermosensitivity of the enzyme. What would be the structural/functional consequences of deleting the βA–βB loop of *Chlamydomonas* Rubisco and inserting the extended C-terminus of *Galdieria partita* (Sugawara *et al.*, 1999).

Galdieria partita Rubisco is a more efficient enzyme than higher plant Rubisco. Would the insertion of the extended C-terminus of *Galdieria partita* Rubisco give catalytic properties comparable to wild-type *Galdieria partita* Rubisco?

6. References

- Andersson, I., (1996). Large structures at high resolution: The 1.6 Å crystal structure of spinach ribulose-1,5-bisphosphate carboxylase/oxygenase complexed with 2-carboxyarabinitol bisphosphate. *J. Mol. Biol.* 259, 160-174.
- Andersson, I., & Brändén, C.I. (1984). Large single crystals of spinach 1,5-bisphosphate carboxylase/ oxygenase suitable for X-ray studies. *J. Mol. Biol.* 172, 363-366.
- Andrews, T.J. (1988). Catalysis by cyanobacterial ribulose-bisphosphate carboxylase large subunits in the complete absence of small subunits. *J. Biol. Chem.* 263, 12213-12219.
- Berglund, G.I., Carlsson, G.H., Smith, A.T., Szöke, H. , Henriksen, A. & Hajdu, J. (2002). The catalytic pathway of horseradish peroxidase at high resolution. *Nature* 417, 463-468.
- Bowes, G., Ogren, W.L. & Hageman, R.H. (1971). Phosphoglycolate production catalyzed by ribulose diphosphate carboxylase. *Biochem. Biophys. Res. Commun.* 45, 716-722.
- Chan, P.H., & Wildman, S.G. (1972). Chloroplast DNA codes for the primary structure of the large subunit of Fraction 1 protein. *Biochim. et Biophys. Acta* 277, 677-680.
- Chen, Z., Chastain, C.J., Al-Abed, S.R., Chollet, R. & Spreitzer R.J. (1988). Reduced CO₂/O₂ Specificity of Ribulose-Bisphosphate Carboxylase/Oxygenase in a Temperature-Sensitive Chloroplast Mutant of *Chlamydomonas*, *Proc. Natl. Acad. Sci. U. S. A.* 85, 4696-4699.
- Chen, Z.X., Hong, S. & Spreitzer, R.J. (1993). Thermal-instability of ribulose-1,5-bisphosphate carboxylase oxygenase from a temperature-conditional chloroplast mutant of *Chlamydomonas-reinhardtii*. *Plant Physiol.* 101, 1189-1194.
- Chen, Z. & Spreitzer, R.J. (1989). Chloroplast intragenic suppression enhances the low CO₂/O₂ specificity of mutant ribulose bisphosphate carboxylase/oxygenase. *J. Biol. Chem.* 264, 3051-3053.
- Chen, Z.X., Yu, W.Z., Lee, J.H., Diao R. & Spreitzer, R.J. (1991). Complementing amino-acid substitutions within loop-6 of the alpha-beta-barrel active-site influence the CO₂/O₂ specificity of chloroplast ribulose-1,5-bisphosphate carboxylase oxygenase. *Biochemistry* 30, 8846-8850.
- Du, Y.C., Hong, S.J. & Spreitzer, R.J. (2000). RbcS suppressor mutations improve the thermal stability and CO₂/O₂ specificity of rbcL-mutant ribulose-1,5-

bisphosphate carboxylase/oxygenase. *Proc. Natl. Acad. Sci. USA* 97, 14206-14211.

Duff, A.P., Andrews, T.J. & Curmi, P.M.G. (2000). The transition between the open and closed states of rubisco is triggered by the inter-phosphate distance of the bound bisphosphate. *J. Mol. Biol.* 298, 903-916.

Ellis, R.J. (1981). Chloroplast proteins: synthesis, transport and assembly. *Annu Rev. Plant Phys.* 32, 111-137.

Flachmann, R. & Bohnert, H.J. (1992). Replacement of a conserved arginine in the assembly domain of Ribulose-1,5-bisphosphate carboxylase/oxygenase small subunit interferes with holoenzyme formation. *J. Biol. Chem.* 267, 10576-10582.

Ferreira, R.B. & Davies, D.D. (1987). Protein degradation in *Lemna* with particular reference to Ribulose bisphosphate carboxylase. II. The effect of nutrient starvation. *Plant Physiol.* 83, 878-883.

Garcia-Ferris, C. & Moreno, J. (1994). Oxidative modification and breakdown of ribulose 1,5-bisphosphate carboxylase/oxygenase induced in *Euglena gracilis* by nitrogen starvation. *Planta* 193, 208-215.

Gutteridge, S. & Gatenby, A.A. (1995). Rubisco synthesis, assembly, mechanism, and regulation. *Plant Cell* 7, 809-819.

Gutteridge, S., Rhoades, D.F. & Herrmann, C. (1993). Site-specific mutations in a loop region of the C-terminal domain of the large subunit of ribulose bisphosphate carboxylase/oxygenase influence substrate partitioning. *J. Biol. Chem.* 268, 7818-7824.

Hansen, S., Burkow, V., Hough, E. & Andersen, K. (1999). The crystal structure of Rubisco from *Alcaligenes eutrophus* reveals a novel central eight-stranded β -barrel formed by β -strands from four subunits. *J. Mol. Biol.* 288, 609-621.

Hong, S. & Spreitzer, R.J. (1997). Complementing substitutions at the bottom of the barrel influence catalysis and stability of ribulose-bisphosphate carboxylase oxygenase. *J. Biol. Chem.* 272, 11114-17.

Harding, M.M. (1999). Geometry of metal-ligands in proteins. *Acta Cryst.* D55, 1432-43.

Hartman, F.C. & Harpel, M.C. (1994). Structure, function, regulation, and assembly of D-ribulose-1,5-bisphosphate carboxylase oxygenase. *Annu. Rev. Biochem.* 63, 197-234.

Kane, H.J., Wilkin, J.M., Portis, A.R. & Andrews T.J. (1998). Potent inhibition of ribulose-bisphosphate carboxylase by an oxidized impurity in ribulose-1,5-bisphosphate. *Plant Physiol.* 117, 1059-1069.

- Kawashima, N. & Wildman, S.G. (1972). Studies of fraction protein IV. Mode of inheritance of primary structure in relation to whether chloroplast or nuclear DNA contains the code for a chloroplast protein. *Biochim. et Biophys. Acta* 262, 42–49.
- King, W.A., Gready, J.E. & Andrews, T.J. (1998). Quantum chemical analysis of the enolization of ribulose biphosphate: The first hurdle in the fixation of CO₂ by Rubisco. *Biochemistry* 37, 15414-15422.
- Lilley, R.M. & Portis, A.R. (1997). ATP Hydrolysis Activity and Polymerization State of Ribulose-1,5-Bisphosphate Carboxylase Oxygenase Activase (Do the Effects of Mg²⁺, K⁺, and Activase Concentrations Indicate a Functional Similarity to Actin?). *Plant Physiol.* 114, 605–613.
- Lorimer, G.H. & Mizioro, H.M. (1980). Carbamate formation on the ε-amino group of a lysyl residue as the basis for the activation of ribulosebisphosphate carboxylase by CO₂ and Mg²⁺. *Biochemistry* 19, 5321–5324.
- Lorimer, G.H. (1981). The carboxylation and oxygenation of ribulose 1,5-bisphosphate: the primary events in photosynthesis and photorespiration. *Annual Review of Plant Physiology* 32, 349–383.
- Moreno, J. & Spreitzer, R.J. (1999). C172S substitution in chloroplast-encoded large subunit affects stability and stressed-induced turn over of Ribulose-1,5-bisphosphate carboxylase/oxygenase. *J. Biol. Chem.* 274, 26789-26793.
- Newman, J. & Gutteridge, S. (1993). The X-ray structure of *Synechococcus* ribulose-bisphosphate carboxylase oxygenase-activated quaternary complex at 2.2-Angstrom resolution. *J. Biol. Chem.* 268, 25876-25886.
- Nienhaus, G.U., Heinzl, J., Huenges, E. & Parak, F. (1989). Protein crystal dynamics studied by time-resolved analysis of X-ray diffuse-scattering. *Nature* 338, 665-666.
- Ogren, W.L. & Bowes, G. (1971). Ribulose diphosphate carboxylase regulates soybean photorespiration. *Nature New Biol.* 230, 159–160.
- Portis, A.R. (1995) The regulation of Rubisco by Rubisco activase. *J. Exp. Bot.* 46, 1285-1291.
- Read, B.A. & Tabita, F.R. (1994). High substrate-specificity factor ribulose-bisphosphate carboxylase oxygenase from eukaryotic marine-algae and properties of recombinant cyanobacterial rubisco containing algal residue modifications. *Arch. Biochem. Biophys.* 312, 210-218.
- Robinson, S.P. & Portis, A.R. (1989). Adenosine triphosphate hydrolysis by purified Rubisco activase. *Arch Biochem. Biophys* 268, 93-99.

Schloss, J.V., Stringer, C.D. & Hartman, F.C. (1978). Identification of essential lysyl and cysteinyl residues in spinach Ribulose biphosphate carboxylase/oxygenase modified by affinity label N-bromoacetyethanolamine phosphate. *J. Biol. Chem.* 253, 5707-5711.

Salvucci, M.E. & Ogren, W.L. (1996). The mechanism of Rubisco activase: Insights from studies of the properties and structure of the enzyme. *Photosynth. Res.* 47, 1-11.

Satagopan, S. & Spreitzer, R.J. (2004). Substitutions at the Asp-473 latch residue of *Chlamydomonas* Ribulosebiphosphate carboxylase/oxygenase cause decrease in carboxylation efficiency and CO₂/O₂ specificity. *J. Biol. Chem.* 279, 14240-44.

Somerville, C.R., Portis, A.R. & Ogren WL. (1982). A mutant of *Arabidopsis thaliana* which lacks activation of RUBP carboxylase in vivo. *Plant Physiol.* 70, 381-387.

Spreitzer, R.J. (1993) Genetic dissection of Rubisco structure and function. *Annu. Rev. Plant Physiol. Plant Mol. Biol.* 44, 411-434.

Spreitzer, R.J. (1998). The molecular biology of chloroplasts and mitochondria in *Chlamydomonas* (Rochaix, J. D., Goldschmidt-Clermont, M., and Merchant, S., eds) pp. 515-527, *Kluwer Academic Publishers*, Dordrecht, Netherlands.

Spreitzer, R.J. & Mets, L. (1981). Photosynthesis-deficient mutants of *Chlamydomonas Reinhattii* with associated light-sensitive phenotypes. *Plant Physiol.* 67, 565-569.

Sugawara, H., Yamamoto, H., Shibata, N., Inoue, T., Okada, S., Miyake, Yokota, A. & Kai, Y. (1999). Crystal Structure of Carboxylase Reaction-oriented Ribulose-1,5-Bisphosphate Carboxylase/Oxygenase from a Thermophilic Red Alga, *Galdieria partita*. *J. Biol. Chem.* 274, 15655-15661.

Taylor, T.C., Backlund, A., Bjorhall, K., Spreitzer, R.J. & Andersson I (2001). First crystal structure of rubisco from a green alga, *Chlamydomonas reinhardtii*. *J. Biol. Chem.* 276, 48159-48164.

Taylor, T.C. & Andersson, I. (1996). Structural transitions during activation and ligand binding in hexadameric Rubisco inferred from the crystal structure of the activated unliganded spinach enzyme. *Nature Struct. Biol.* 3, 95-101.

Taylor, T.C. & Andersson, I. (1997) The structure of the complex between rubisco and its natural substrate ribulose 1,5-bisphosphate. *J. Mol. Biol.* 265, 432-444.

Taylor, T.C. & Andersson, I. (1997) Structure of a product complex of spinach ribulose 1,5-bisphosphate carboxylase/oxygenase. *Biochemistry* 36, 4041-4046.

Taylor, T.C., Fothergill, M.D. & Andersson, I. (1997) A common structural basis for the inhibition of Ribulose 1,5-bisphosphate carboxylase by 4-carboxyarabinitol 1,5-bisphosphate and xylulose 1,5-bisphosphate. *J. Biol. Chem.* 271, 32894-32899.

Wang, Z.Y., Ramage, R.T. & Portis, A.R. (1993). Mg^{2+} and ATP or adenosine 5'-[γ -thio]-triphosphate(ATPgS) enhances intrinsic fluorescence and induces aggregation which increases the activity of spinach Rubisco activase. *Biochim. Biophys. Acta* 1202: 47-55.

Wasmann, C.C, Ramage, R.T., Bohnert, H.J. & Ostrem, J.A. (1989). Identification of an assembly domain in the small subunit of Ribulose-1,5-bisphosphate carboxylase. *Proc. Natl. Acad. Sci. U.S.A.* 86, 1198-1202.

Whitney, S.M. & Andrews, T.J. (1998). The CO_2/O_2 specificity of single-subunit ribulose-bisphosphate carboxylase from the dinoflagellate, *Amphidinium carterae*. *Aust. J. Plant Physiol.* 25, 131-138.

Acknowledgements

The production of this thesis is culmination of several years of work, which could not have been possible without the support of many people.

I would like to gratefully acknowledge my supervisor, Professor Inger Andersson, without whose dedication and unreserved support this work could never have been completed. Inger, you are a true scientist and a great person and I could not imagine a better advisor during my graduate studies.

Tom, my co supervisor, thanks for all the support and encouragements and patience during these years.

I would also like to thank:

Anke for taking me to the world of crystallography in the early days and answering all my questions

David without whose help I would have been a blind in the world of computer. Thank you also Erling and Remco for all the help with computer related problems.

My summer student, Andreas Cederlund for helping me to grow crystals of Rubisco mutants.

Our Collaborator, Professor Bob Spreitzer at the University of Nebraska, for his interest in this work and for providing us with Rubisco mutant cells.

The present and former members of the crystallography lab (SLU or Uppsala University). Thank you all for making this place such a wonderful place to work in.

Finally, I would like to thank my wife Faranak and my children Behrad and Vida. Thank you guys for bringing so much joy into my life and for making me feel loved and special, Faranak, thanks for inspiration, support and patience especially during these past few weeks.